Radiol med (2015) 120:959–966
DOI 10.1007/s11547-014-0474-0

MAGNETIC RESONANCE IMAGING

Accuracy of MRI for the diagnosis of metastatic cervical lymphadenopathy in patients with thyroid cancer

Qinghua Chen · Prashant Raghavan · Sugoto Mukherjee · Mark J. Jameson · James Patrie · Wenjun Xin · Junfang Xian · Zhenchang Wang · Paul A. Levine · Max Wintermark

Received: 21 April 2014 / Accepted: 16 June 2014 / Published online: 1 March 2015

Abstract
Purpose The aim of this study was to systematically compare a comprehensive array of magnetic resonance (MR) imaging features in terms of their sensitivity and specificity to diagnose cervical lymph node metastases in patients with thyroid cancer.
Materials and methods The study included 41 patients with thyroid malignancy who underwent surgical excision of cervical lymph nodes and had preoperative MR imaging ≤4weeks prior to surgery. Three head and neck neuroradiologists independently evaluated all the MR images. Using the pathology results as reference, the sensitivity, specificity and interobserver agreement of each MR imaging characteristic were calculated.
Results On multivariate analysis, no single imaging feature was significantly correlated with metastasis. In general, imaging features demonstrated high specificity, but poor sensitivity and moderate interobserver agreement at best.
Conclusions Commonly used MR imaging features have limited sensitivity at correctly identifying cervical lymph node metastases in patients with thyroid cancer. A negative neck MR scan should not dissuade a surgeon from performing a neck dissection in patients with thyroid carcinomas.

Keywords Thyroid cancer · Neck dissection · Metastatic lymph nodes · MRI · Accuracy

Q. Chen · P. Raghavan · S. Mukherjee · M. Wintermark (✉)
UVA Department of Radiology, Neuroradiology Division, University of Virginia, Box 800170, Charlottesville, VA 22908, USA
e-mail: Max.Wintermark@gmail.com

Q. Chen · J. Xian · Z. Wang
Department of Radiology, Beijing Tongren Hospital, Capital Medical University, Beijing, China

M. J. Jameson · P. A. Levine
Department of Otolaryngology – Head and Neck Surgery, University of Virginia, Charlottesville, VA, USA

J. Patrie · W. Xin
Department of Public Health Sciences, University of Virginia, Charlottesville, VA, USA

M. Wintermark
Department of Radiology, Centre Hospitalier Universitaire Vaudois, Lausanne, Switzerland

Introduction

In patients with thyroid cancer, the presence of cervical nodal metastasis, a relatively common finding, is a negative prognostic indicator in patients older than 45 years of age and significantly impacts therapy. Thus, the identification of cervical nodal metastasis by preoperative imaging plays a key role in treatment planning for thyroid cancer. Given the concerns regarding evaluating patients with contrast-enhanced computed tomography (CT) due to iodinated contrast interfering with radioactive iodine uptake, alternative imaging approaches have been recommended including neck ultrasonography and magnetic resonance (MR) imaging. When assessing for cervical nodal metastasis, MRI may have advantages over ultrasonography because of its ability to assess retrosternal and retropharyngeal lymph nodes, which cannot be evaluated by ultrasonography.

A number of investigations have been performed regarding the MR imaging features of lymph nodes harbouring metastatic cancer, e.g. size, shape, necrosis, T1 and T2 signal intensity, enhancement, etc. [1–14]. However, few studies have evaluated the characteristics of metastatic thyroid

cancer and MR imaging features have not been compared to each other either alone or in aggregate in terms of their accuracy to predict metastatic involvement. The goal of our study was to systematically evaluate all previously reported MR imaging features in terms of their diagnostic accuracy for cervical lymph nodal metastasis in patients with thyroid cancer.

Materials and methods

Study design

With the approval of the University of Virginia Institutional Review Board who granted us a waiver of consent, we retrospectively reviewed medical records for all patients with a diagnosis of thyroid malignancy who underwent surgery in the Department of Otolaryngology—Head and neck Surgery from June 2004 through March 2011. Of the 193 patients who met these criteria, 41 patients fulfilled the following inclusion criteria: (1) confirmed tissue diagnosis of thyroid cancer, (2) lateral and/or central compartment neck dissection completed and pathology results reported by level, and (3) preoperative MR imaging performed at UVA within 4 weeks prior to neck dissection. At UVA, all head and neck surgeons remove neck dissection specimens en bloc and place these specimens on a "neck board" that visually isolates the nodes at each level for histopathologic review. The neck board bearing the neck dissection specimen is transported to Surgical Pathology for processing where the specimen is divided into nodal levels based on its position on the board. Each node at each level is then evaluated using a standard histopathological approach. While this process is performed routinely and consistently, it has the potential to introduce some error in nodal level designation as compared to imaging. This issue was addressed in the statistical analysis as described below.

MR imaging and image review

All study patients underwent MR imaging preoperatively. The MR studies were performed on a 1.5 T MR scanner with a head coil using the following pulse sequences: axial and coronal T1-weighted images, axial fat-sat T2-weighted images, and gadolinium-enhanced fat-suppressed axial and coronal T1-weighted images.

For this study, three neuroradiologists specialised in head and neck imaging independently evaluated the MR images. The radiologists were blinded to each other, to the clinical information except for the presence of thyroid cancer, to the original clinical interpretation of MR studies, and to the neck dissection results.

The reviewers assessed the quality of MR images as good (2), intermediate (1), or poor (0). The observers reviewed all visible lymph nodes in all 41 patients. For each lymph node, they characterised as series of MR imaging features, including exaggerated enhancement, signal on T1-weighted images, signal on T2-weighted images, node shape, node size Y, node size X, node size Z, edge, vascular encasement, and necrosis.

It was not possible to match exactly the lymph nodes characterised on imaging and the lymph nodes resected during surgery. For this reason, we did not perform a node-by-node comparison, but rather level-by-level (levels I–VII) and neck-by-neck (right lateral nodes, left lateral nodes and central compartment nodes) comparisons between imaging and histology, as detailed below.

Each level in each patient was assigned a single value for each imaging feature. If at least one lymph node in a specific level exhibited a given feature, the entire level was considered to be positive for that feature. For node size, the dimensions of the largest node of the level were recorded for that level. For levels that did not show any lymph nodes, the size recorded was zero, and the imaging features listed above were all considered negative.

A similar approach was used for the histology: a level was considered positive if any node within the level exhibited metastatic cancer on histopathology, and the level was considered negative if all the nodes at within the level were free of cancer.

Using the histology as a reference standard, we first performed a "strict level-by-level" analysis, comparing each level in each patient on imaging and on histology. Given the possible variability in surgical and pathological assignment of nodal levels (see above), a "lenient level-by-level" analysis was also performed, which considered that an abnormal lymph node noted on imaging in one level may have been surgically assigned to an adjacent level, e.g. a node in low level II on imaging that was sent to pathology as a level III node intraoperatively. Finally, we performed a "neck-by-neck" analysis, dividing the levels in each patient into right neck (levels Ia, Ib, IIa, IIb, III, IV and V), a left neck (levels I–V) and a central neck (levels VI and VII). Finally, we calculated interobserver agreement for the statistically significant imaging features.

Statistical analyses

Strict level-by-level analyses

The goal of the analyses was to determine if there were imaging characteristics for each level that could be utilised as potential markers for the identification of lymph nodes with metastasis at each neck level in patients with thyroid cancer.

Outcome variable The outcome variable for this set of analyses was a binary indicator variable (i.e. 0 or 1) for each level based that was assigned the value 1 if any one lymph node at a particular level was positive on histopathology. Conversely, if all the lymph nodes at a particular level were negative on histopathology, the binary variable was assigned the value 0.

Predictor variables The imaging characteristics assessed as potential markers for the identification of metastatic lymph node levels in patients with thyroid cancer were exaggerated enhancement, signal on T1-weighted images, signal on T2-weighted images, node shape, node size Y, node size X, node size Z, edge, vascular encasement, and necrosis.

Analyses Binomial univariate analyses followed by a multivariate generalised estimating equation (GEE) regression model were utilised to examine whether one or more of the aforementioned imaging characteristics were associated with histopathology. It is important to note that, unlike traditional logistic regression, which is commonly utilised to analyse partial associations between a binary outcome variable and a set of predictor variables, the GEE model provides accurate regression parameter estimates even when the binary outcome data cannot be presumed to be uncorrelated, which in the present case is unlikely to be true, since multiple lymph node levels were examined per patient. The GEE regression model variance and covariance parameters that were utilised in hypothesis testing were estimated via the Huber and White sandwich estimator assuming within cluster measurement dependence [15].

Hypothesis testing With regard to hypothesis testing, the GEE modified version of the Type III Wald Chi square statistic was utilised to test for significant partial associations between histopathology and imaging characteristics. A $p \leq 0.05$ decision rule was established a priori as the null hypothesis (i.e. no partial association) rejection criterion. Reported predicted probabilities for a positive metastatic lymph node histopathology classification were calculated based on the inverse-logit transformation of the GEE multivariate regression model logit predictions.

Lenient level-by-level analyses The level-by-level analysis was repeated allowing for discrepancies in the definition of the levels between imaging and surgery. More specifically, we repeated the analysis described above, this time considering that each of the levels was positive on histology if it contained a positive lymph node or if any of its immediate neighbour contained at least one positive lymph node. For example, if level III contained a pathological node, both levels II and IV were considered positive. This lenient level-by-level analysis was designed to yield the best-case scenario results in terms of the accuracy of imaging, whereas the strict level-by-level analysis was designed to yield the worse case scenario results.

"Neck-by-neck" analyses The diagnostic agreement analyses, when conducted based on the "neck" classification (right neck, left neck and central neck), were carried out in exactly the same way as the diagnostic agreement analyses conducted based on the "level" classification.

Interobserver agreement analyses The analyses described above were conducted independently for the three reviewers, and the results are reported in the tables as the range of values for the three reviewers, to demonstrate the interobserver variability. In addition, interobserver agreement was calculated using kappa statistics. Statistical significance was set at 0.05.

Statistical software The GENMOD procedure of SAS version 9.2 (SAS, Institute Inc., Cary, NC) was utilised to conduct the GEE regression analysis and the software of Spotfire Splus 8.2 (TIBCO Inc, Palo Alto, CA) was utilised to conduct the diagnostic agreement analyses.

Results

Study patients

A total of 193 patients were considered for enrolment in this study. Forty-nine of the 193 patients had undergone the required preoperative MR scan and 41 out of these 49 met all the other inclusion criteria. The 41 patients included 14 males and 27 females with a median age of 54.0 (range 17–90 years). The 41 patients in the study cohort represent 492 total neck levels (205 left, 205 right, and 82 central) of which 260 levels demonstrated no nodes on MR imaging. Thus, 232 lymph node levels were evaluated by MR imaging. The types of thyroid cancer and lymph node status for each are summarised in Table 1.

The total number of lymph nodes that were surgically excised and underwent histopathological examination was

Table 1 Distribution of lymph node status by thyroid cancer histological subtype

Thyroid cancer type	Lymph node pathology+	Lymph node pathology−	Total
Papillary	26 (76 %)	8 (24 %)	34
Papillary, follicular variant	2 (50 %)	2 (50 %)	4
Follicular	0 (0 %)	2 (100 %)	2
Medullary	0 (0 %)	1 (100 %)	1
Total	28 (68 %)	13 (32 %)	41

1,304; of these, 196 harboured metastasis and 1,108 were negative. A total of 164 levels contained lymph nodes at pathology, while 58 levels did not. Of these 164 levels, 79 levels were positive for thyroid cancer metastasis on pathology, while 85 were negative (Table 2).

Imaging studies

All patients underwent T1- and T2-weighted sequences and post-contrast T1 imaging, except for one patient without post-contrast imaging. The MR imaging quality as assessed by the three reviewers is reported in Table 3. Overall, post-contrast images were of lower quality than pre-contrast images.

Strict level-by-level analysis

In the univariate analyses (Table 4), the strict level-by-level analysis identified a number of MR imaging characteristics that were significantly correlated with the presence of metastatic disease: conglomerated lymph nodes, node size, T1 signal, exaggerated enhancement, shape, as well as necrosis and encasement (Figs. 1, 2, 3). In general, these features demonstrated high specificity, but poor sensitivity and moderate interobserver agreement at best (Table 4). In the multivariate analysis, no single MR imaging feature was independently significant; however, a model built from all the features included in the multivariate analysis was significantly correlated ($p < 0.05$) with the presence of metastatic disease. The overall accuracy across the three readers was similar and ranged from 49 to 56 %.

Table 2 Pathological results by neck and level

	Total	Pathology+	Pathology−
Necks			
Lateral	156	73 (47 %)	83 (53 %)
Left Side	79	36 (45 %)	43 (55 %)
Right Side	77	37 (48 %)	40 (52 %)
Central	8	6 (75 %)	2 (25 %)
Total	164	79 (48 %)	85 (52 %)
Levels			
Level I	4	0 (0 %)	4 (100 %)
Level II	31	15 (48 %)	16 (52 %)
Level III	31	18 (58 %)	13 (42 %)
Level IV	26	8 (31 %)	18 (69 %)
Level V	24	7 (29 %)	17 (71 %)
Level VI	44	28 (64 %)	16 (36 %)
Level VII	4	3 (75 %)	1 (25 %)
Total	164	79 (48 %)	85 (52 %)

Lenient level-by-level analysis and neck-by-neck analysis

The lenient level-by-level comparison yielded similar results to the strict level-by-level analysis, suggesting that errors in level identification in the operating room and surgical pathology have little impact on the correlation between imaging finding and histologically proven metastatic disease. For the lenient level-by-level and the neck-by-neck analyses, no single feature remained independently significant in the multivariate analyses. As for the strict level-by-level approach, the models built from all the features included in the multivariate analysis were significantly correlated with the presence of metastasis. The overall accuracy was similar across the three readers for both the lenient level-by-level analysis (49–55 %) and the neck-by-neck analysis (51–55 %).

Multivariate model

The multivariate model including all imaging features (conglomerated lymph nodes, node size, T1 signal, exaggerated enhancement, shape, as well as necrosis and encasement) had an overall sensitivity and specificity of 33–56 % and 90–93 %, respectively. Had such a model been employed in the assessment of these 41 patients, 13 of 14 unnecessary neck dissections would have been avoided, but 12–18 (depending on the reviewer) of 27 positive necks would have been undertreated.

Table 3 MR imaging quality

Image quality	Axial T1		Axial T2 fat sat		Coronal T1		Post-contrast axial T1 fat sat		Post-contrast coronal T1 fat sat	
	Cases	%	Cases	%	Cases	%	Cases	%	Cases	%
2	26	65.00	23	57.50	20	50.00	6	15.00	4	10.00
1	14	35.00	17	42.50	20	50.00	34	85.00	34	85.00
0	0	0.00	0	0.00	0	0.00	0	0.00	2	5.00
Total	40*		40*		40*		40*		40*	

2-Good quality, 1-intermediate quality, 0-poor quality

*Only 40 patients (out of our 41 study patients) received gadolinium contrast for their preoperative MR imaging, and contrast enhancement could only be assessed in the levels of this subset of 40

Table 4 MR imaging features of the cervical lymph nodes

Features	Total	Pathology+	Pathology−	Range of *P* values from the 3 reviewers	Range of sensitivities for the 3 reviewers (%)	Range of specificities for the 3 reviewers (%)	Range of inter-observer agreement (kappa)
Conglomerated lymph nodes	232	81	151	0.001–0.049	6.5–8.5	99.3–99.8	0.43–0.57
Yes	31	27	4				
No	201	54	147				
Maximal node size [1–3, 10, 13, 14]				0.004–0.017	9–11.5	98.9–99.9	0.44–0.59
Axial short diameter		11.9 ± 7.5	6.3 ± 2.2				
Axial long diameter		15.9 ± 8.6	9.4 ± 3.0				
Coronal long diameter		19.1 ± 12.8	11.0 ± 4.3				
Signal on T1[b] [14]	232	81	151	0.001–0.026	12.5–27	96.5–99.3	0.34–0.48
Hetero	16	12	4				
Hyper	87	50	37				
Inter	119	18	101				
Hypo	10	1	9				
Signal on T2[b] [2, 5, 14]	232	81	151	0.340–0.658	21.5–31.5	90.1–94.7	0.27–0.46
Hetero	44	32	12				
Hyper	185	48	137				
Inter	3	1	2				
Hypo	0	0	0				
Necrosis [1–3, 6–11, 13, 14]	232	81	151	0.001–0.415	2–15.5	99–99.7	0.40–0.53
Definitive	12	10	2				
Possible	25	20	5				
No	195	51	144				
Exaggerated enhancement [5, 13, 14]	231	81	150	0.001–0.010	14.5–19.5	98.7–98.8	0.38–0.52
Yes	83[a]	59	24				
No	148[a]	22	126				
Shape [8, 10, 13, 14]	232	81	151	0.001–0.005	11.5–27	96.7–99.2	0.41–0.54
Normal	132	19	113				
Spherical/irregular	100	62	38				
Edge [9, 13, 14]	232	81	151	0.001–0.634	2–15.5	99.4–99.8	0.45–0.51
Smooth	187	44	143				
Blurred/indistinct/spiculated	45	37	8				
Vascular encasement [2]	232	81	151	0.001–0.591	1–10.5	99.5–100	0.42–0.59
Yes	16	14	2				
No	216	67	149				

[a] Only 40 patients (out of our 41 study patients) received gadolinium contrast for their preoperative MR imaging, and contrast enhancement could only be assessed in the levels of this subset of 40 patients. The patient without gadolinium administration has only one negative lymph node in right level two in bilateral neck

[b] Signal on T1- or T2-weighted images were assessed by comparing with the corresponding intensity of the sternocleidomastoid muscle

Discussion

Preoperative evaluation of thyroid cancer has conventionally included ultrasound of the neck to detect metastatic lymph nodes. Ultrasonography is inexpensive, easily performed and can be accurate in prediction of lymph node metastasis [16], especially in the lateral neck. The addition of contrast-enhanced CT may enable detection of lymph

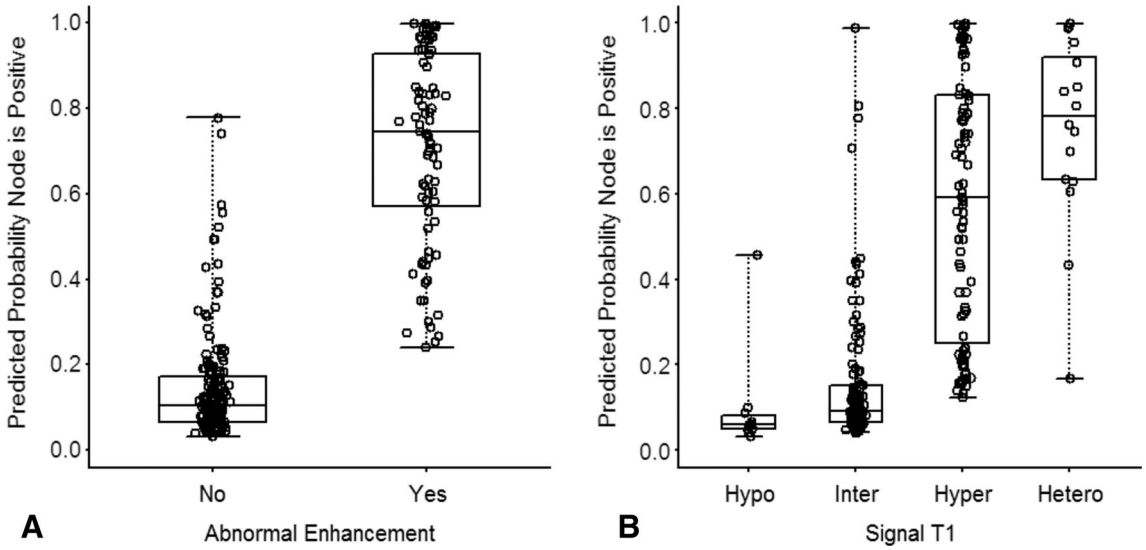

Fig. 1 Predicted values of the significant imaging characteristics of lymph nodes for positive pathology in patients with thyroid cancer

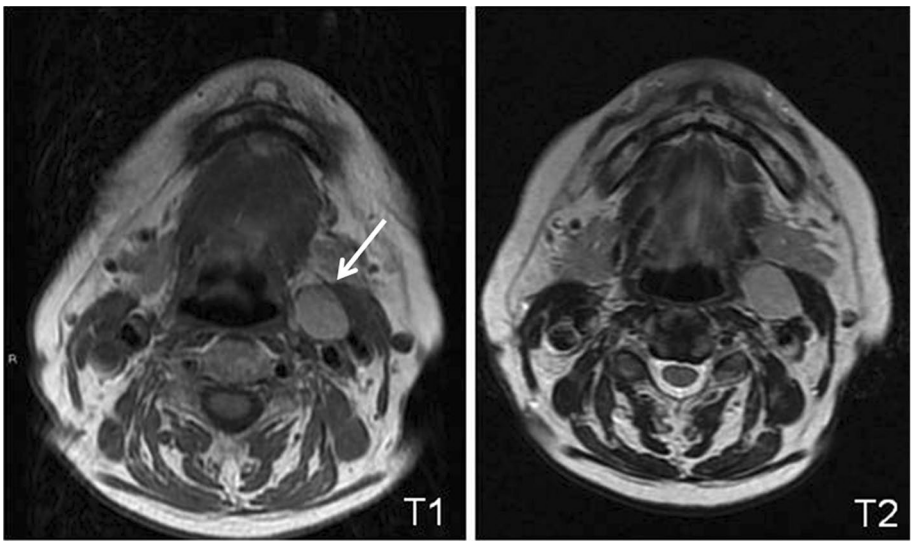

Fig. 2 Example of a metastatic, T1 hyperintense left level II lymph node (*arrow*) in a patient with papillary thyroid cancer. The node is also hyperintense on the T2-weighted image. The T1 hyperintensity is likely due to the presence of thyroglobulin within the metastatic lymph node

nodes not easily accessed by ultrasound such as in the central compartment [17]. However, preoperative contrast-enhanced CT is discouraged in patients with differentiated thyroid carcinomas due to the concern that intravenous iodinated contrast agent could affect radioactive iodine uptake for months, thus interfering with postoperative radioiodine therapy [18].

The other imaging options available include contrast-enhanced MR imaging and fluorodeoxyglucose positron emission tomography (FDG-PET) imaging. The latter is best used in surveillance of treated thyroid malignancy especially in a setting of rising thyroglobulin levels when conventional radioiodine nuclear imaging and ultrasound are negative [19]. In studies by Choi et al. [20] and Jeon et al. [21], PET–CT did not appear to confer a significant advantage over ultrasound or CT in the preoperative evaluation of lymphadenopathy from thyroid cancer.

MR imaging, with its multiplanar capability and superior soft tissue resolution, appears to be an attractive alternative. MR imaging also has the ability to image areas inaccessible by ultrasound such as the mediastinum and retropharyngeal region. Also, gadolinium-based contrast medium does not interfere with future radioiodine administration [22].

Our study evaluated multiple imaging features of lymph nodes that have been previously reported as imaging predictors of lymph node metastasis. None of the individual features allowed for reliable identification of metastatic lymph nodes; the features were specific, but not sensitive. Takashima et al., in a series of 34 patients with papillary thyroid cancer who underwent MR imaging, were able to identify metastatic

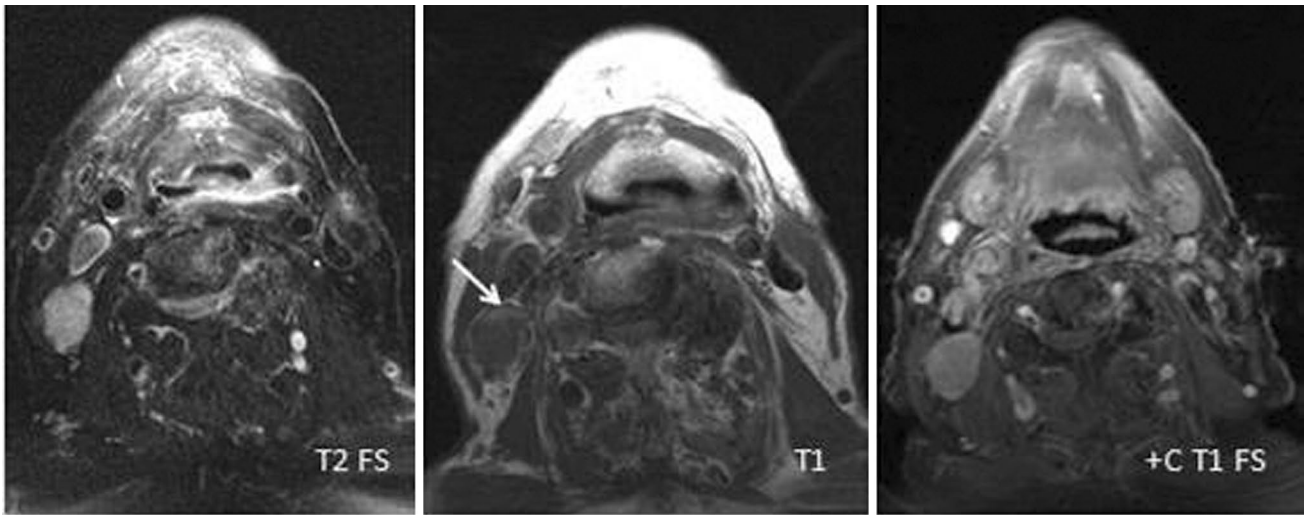

Fig. 3 Metastatic right level III lymph node from a papillary thyroid cancer. This node shows heterogenous intensity, and is hyperintense along its anterior aspect (*arrow*) on the T1-weighted images. It is hyperintense on the fat-saturated T2-weighted image. It demonstrates homogeneous enhancement on the post-contrast fat-suppressed T1-weighted image

lymph nodes with a sensitivity of only 41 % using the presence of cystic change and a size cut off of 13 mm [23]. In a series of 26 patients with thyroid cancer studied by Gross et al., using the criteria of nodal size, T2 signal, cystic change and compression of adjacent structures, the average overall percent sensitivity, specificity, positive predictive value, negative predictive value, and accuracy of MR imaging were 95, 51, 84, 78, and 83 %, respectively. The authors recommended that MR imaging not be used as a screening tool given its low specificity [2]. Our study is in agreement with these and indicates that using individual MR imaging characteristics is not sufficiently sensitive to determine the presence of metastatic disease; an MR study that shows none of the features of the combined model (e.g. no conglomerated lymph nodes, no nodes greater than 10 mm in their short diameter, no increased T1 signal intensity, no exaggerated enhancement, normal node shape, no necrosis and no encasement) is associated with a low likelihood that metastatic thyroid cancer is present.

The interobserver agreement for the different imaging features was moderate at best, reflecting the subjectivity in the assessment in some of these features. The THREE neuroradiologists who reviewed the study images were specialised in head and neck imaging, and they originally agreed on criteria to assess the different imaging features before reviewing the imaging studies independently.

Of note, our results apply mainly to papillary thyroid carcinomas, as these constituted the large majority of our study population. Papillary thyroid carcinomas are the most frequent type of thyroid cancer and tend to spread to lymph nodes more so than the other types of thyroid cancers, making the issue of imaging diagnosis of metastatic lymph nodes in patients with papillary thyroid cancer particularly relevant.

The quality of contrast-enhanced MR imaging was less than other sequences, most likely because these were the last sequences obtained and are therefore prone to motion artefacts.

We acknowledge several limitations to our study. The study population was small. It was impossible to exactly match the lymph nodes on MR imaging and histopathology. For practical purposes, we had to consider a level positive when any node in this level was positive on histopathology. This may have resulted in an overestimation of the sensitivity of the imaging findings. However, since none of the imaging features had a particularly high sensitivity, this was not an issue.

In conclusion, individual MR imaging characteristics have limited sensitivity at identifying metastatic lymph nodes in patients with thyroid cancer. A negative neck MR scan should not dissuade a surgeon from performing a neck dissection in patients with thyroid carcinomas. Future studies should assess the diagnostic accuracy of advanced MR imaging sequences such as diffusion- and perfusion-weighted imaging.

Conflict of interest The authors have no disclosure.

Ethical standards Ethical standards were respected and the Institute/Hospital Ethical Review Board has approved the study.

References

1. van den Brekel MW, Stel HV, Castelijns JA et al (1990) Cervical lymph node metastasis: assessment of radiologic criteria. Radiology 177:379–384

2. Gross ND, Weissman JL, Talbot JM et al (2001) MRI detection of cervical metastasis from differentiated thyroid carcinoma. Laryngoscope 111:1905–1909
3. Feinmesser R, Freeman JL, Noyek AM, Birt BD (1987) Metastatic neck disease. A clinical/radiographic/pathologic correlative study. Arch Otolaryngol Head Neck Surg 113:1307–1310
4. Mizowaki T, Nishimura Y, Shimada Y et al (1996) Optimal size criteria of malignant lymph nodes in the treatment planning of radiotherapy for esophageal cancer: evaluation by computed tomography and magnetic resonance imaging. Int J Radiat Oncol Biol Phys 36:1091–1098
5. Krestan C, Herneth AM, Formanek M, Czerny C (2006) Modern imaging lymph node staging of the head and neck region. Eur J Radiol 58:360–366
6. Friedman M, Shelton VK, Mafee M et al (1984) Metastatic neck disease. Evaluation by computed tomography. Arch Otolaryngol Head Neck Surg 110:443–447
7. Stevens MH, Harnsberger R (1988) Computed tomography in evaluating metastatic neck disease. Arch Otolaryngol Head Neck Surg 114:1041
8. Close LG, Merkel M, Vuitch MF et al (1989) Computed tomographic evaluation of regional lymph node involvement in cancer of the oral cavity and oropharynx. Head Neck 11:309–317
9. Mancuso AA, Maceri D, Rice D, Hanafee W (1981) CT of cervical lymph node cancer. AJR Am J Roentgenol 136:381–385
10. Som PM (1987) Lymph nodes of the neck. Radiology 165:593–600
11. King AD, Tse GM, Ahuja AT et al (2004) Necrosis in metastatic neck nodes: diagnostic accuracy of CT, MR imaging, and US. Radiology 230:720–726
12. Som PM (1992) Detection of metastasis in cervical lymph nodes: CT and Mr criteria and differential diagnosis. AJR Am J Roentgenol 158:961–969
13. de Bondt RB, Nelemans PJ, Bakers F et al (2009) Morphological MRI criteria improve the detection of lymph node metastases in head and neck squamous cell carcinoma: multivariate logistic regression analysis of MRI features of cervical lymph nodes. Eur Radiol 19:626–633
14. Huber PJ (1965) The behaviour of maximum likelihood estimates under nonstandard conditions. Proc Fifth Berkeley Symp Math Stat Probab 1:221–233
15. White H (1982) Maximum likelihood estimation of misspecified models. Econometrica 50:1–25
16. Park JS, Son KR, Na DG et al (2009) Performance of preoperative sonographic staging of papillary thyroid carcinoma based on the sixth edition of the AJCC/UICC TNM classification system. AJR Am J Roentgenol 192:66–72
17. Choi JS, Kim J, Kwak JY et al (2009) Preoperative staging of papillary thyroid carcinoma: comparison of ultrasound imaging and CT. AJR Am J Roentgenol 193:871–878
18. Amdur RJ, Mazzaferri EL (2005) Intravenous iodinated contrast effects iodine uptake for months. In: Amdur RJ, Mazzaferri EL (eds) Essentials of thyroid cancer management, 1st edn. Springer, New York, pp 211–213
19. Johnson NA, LeBeau SO, Tublin ME (2011) Imaging surveillance of differentiated thyroid cancer. Radiol Clin N Am 49:473–487
20. Choi WH, Chung YA, Han EJ et al (2011) Clinical value of integrated [18f]fluoro-2-deoxy-D-glucose positron emission tomography/computed tomography in the preoperative assessment of papillary thyroid carcinoma: comparison with sonography. J Ultrasound Med 30:1267–1273
21. Jeong HS, Baek CH, Son YI et al (2006) Integrated 18f-fdg pet/ct for the initial evaluation of cervical node level of patients with papillary thyroid carcinoma: comparison with ultrasound and contrast-enhanced CT. Clin Endocrinol 65:402–407
22. Christensen CR, Glowniak JV, Brown PH, Morton KA (2000) The effect of gadolinium contrast media on radioiodine uptake by the thyroid gland. J Nucl Med Technol 28:41–44
23. Takashima S, Sone S, Takayama F et al (1998) Papillary thyroid carcinoma: MR diagnosis of lymph node metastasis. AJNR Am J Neuroradiol 19:509–513